NASA DEVELOP National Program
Alabama – Marshall
Summer 2022

Bhutan Agriculture II

Creating a Graphical User Interface, Crop Mask, and Data Collection Protocol for Analysis of Rice Crop in Bhutan using Remotely Sensed Data

DEVELOP Technical Report
Final Draft- August 9th, 2022

Wangdrak Dorji (Co-Lead)
Tenzin Wangmo (Co-Lead)
Sonam Seldon Tshering
Karma Thinley Dorjee

Advisors:
Tim Mayer, NASA SERVIR Science Coordination Office (Science Advisor)
Filoteo Gomez-Martinez, NASA SERVIR Science Coordination Office (Science Advisor)
Biplov Bhandari, NASA SERVIR Science Coordination Office (Science Advisor)
Meryl Kruskopf, NASA SERVIR Science Coordination Office (Science Advisor)
Stephanie Jimenez, NASA SERVIR Science Coordination Office (Science Advisor)
Kaitlin Walker, NASA SERVIR Science Coordination Office (Science Advisor)
Micky Maganini, NASA SERVIR Science Coordination Office (Science Advisor)
Sean McCartney, NASA Goddard Space Flight Center (Science Advisor)
Kenton Ross, NASA Langley Research Center (Science Advisor)
Robert Griffin, The University of Alabama Huntsville (Science Advisor)
Jeffry Luvall, NASA Marshall Space Flight Center (Science Advisor)

Previous Contributors:
Sherab Dolma
Kusal Khandal
Yeshey Seldon

1. Abstract

Agriculture is an important sector in Bhutan; accounting for 19.2% of Bhutan's GDP in 2020 while also providing livelihoods for approximately 57% of the population. The Department of Agriculture (DoA) in Bhutan still relies on in-field reporting for crop monitoring which is time-consuming and labor intensive. To promote efficiency, the team partnered with the DoA, the Bhutan Foundation, and the Ugyen Wangchuck Institute of Conservation and Environmental Research (UWICER). With the help of science advisors from NASA SERVIR, the team expanded the crop mask, created in the previous term, to the whole country of Bhutan for the time period of 2015–2020 (May–October) and streamlined the sampling protocols for applicability to any available crop data. The random forest model also had pre-processed rice points from Collect Earth Online (CEO) for five heavy rice production dzongkhags: Paro, Samtse, Sarpang, Punakha, and Wangdue Phodrang. The team also developed a graphical user interface (GUI) which provided a visual representation of current trends and rice distribution across Bhutan. The team utilized NASA Earth observations, including Landsat 5 Thematic Mapper (TM), Landsat 7 Enhanced Thematic Mapper Plus (ETM+), Landsat 8 Operational Land Imager (OLI), and Shuttle Radar Topography Mission (SRTM), as well as other Earth observations including Sentinel-1 C-band Synthetic Aperture Radar (C-SAR). This project refined the previous term's methodology to help supplement crop monitoring and increase the frequency of data collected to aid the decision-making process with the use of remote sensing data. The accuracy and kappa score for the testing data were 85.9% and 71.8% respectively.

Key Terms

Remote Sensing, Earth observations, Google Earth Engine, Collect Earth Online, crop mask, rice plantation, Random Forest, graphical user interface

2. Introduction

2.1 Background Information

Bhutan is a small kingdom in Southeast Asia located at the foothills of the eastern Himalayas with a geographical size of 38,394 km² and a population of 771,612 as of 2020 (The World Bank, 2022). In this compact land with a population of less than 800,000, 57% of the Bhutanese population depend on agriculture for their livelihood (World Bank, 2017). Agriculture also plays an important role in the economy of Bhutan; its share in the Gross Domestic Product (GDP) of the country was 19.2% in 2020 (The World Bank, n.d.). According to the Department of Agriculture (DoA), rice is a crucial staple food for the people in the country. The harvested area of rice paddy fields in 2020 was a total of 31,328.42 acres where 30,641.42 acres of the paddy fields were irrigated and the rest were upland producing 53,360.93 MT and 727.48 MT, respectively (Tobden et al., 2021).

With the presence of the Himalayas, Bhutan sits at a high altitude where steep and irregular mountains and varying topography severely limit cultivable land to just 2.46% of the nation's overall area (Macrotrends, n.d.). The country faces many challenges in creating, maintaining, and monitoring agricultural lands due to natural geological limitations, and national farming efforts are now being further hindered by shifting climate variabilities. Rising seasonal temperatures and precipitation threaten rice crops nationwide (Parker et al., 2017). Among the many

challenges that are faced by the farmers in Bhutan, weed and pest management are the main constraints with rice productivity, along with soil nutrient management. Insect pests, mainly armyworms (*Pseudaletia separata*), have had severe outbreaks in some years, and wildlife, primarily wild boars, act as vertebrate pests of agricultural crops in Bhutan (NPPC, n.d).

The DoA depends on the field reports and surveys of different crops for the development of national statistics which are helpful for decision-making processes. The surveys are a set of questionnaires that are disseminated to rural households in all 205 Gewogs in the 20 districts of the country. Thorough field surveys are hindered by the mountainous topography, and the survey strategy faces difficulties producing precise survey locations and identifying unbiased plot sizes for field reporting (Tobden et al., 2021). In-field crop monitoring is also time-consuming and labor intensive.

The previous Bhutan Agriculture I team (Dolma et al., 2021) from NASA DEVELOP created a crop mask for June to October of 2020 using NASA and European Space Agency (ESA) Earth observations to identify and monitor areas of rice cultivation in the districts of Paro, Punakha, Samtse, Sarpang, Trongsa, Zhemgang, Wangdue Phodrang, and Samdrup Jongkhar. The team also provided the partners with a sampling protocol to replicate the team's methods of identifying rice paddy fields and generating a crop mask. This expanded the DoA's capacity to integrate NASA and ESA Earth observation data into their crop monitoring methods to aid national crop management. Building upon the previous term's work, the Bhutan Agriculture II team utilized the same NASA and ESA Earth observations but applied terrain correction to remove noise from the existing datasets and also computed additional indices that highlight vegetation phenology and manmade development changes for classifying rice. With the help of science advisors from NASA SERVIR, the team expanded the original crop mask to the whole country of Bhutan. The team also worked to streamline the sampling protocols from the previous term for applicability to any available crop data and created a Graphic User Interface (GUI) to provide visual representation of the current trends in rice distribution across Bhutan.

The team expanded the Random Forest (RF) model to the whole country and made the GUI for the whole country, but for the initial data collection the team focused on five districts with heavy rice production: Samtse, Paro, Punakha, Wangdue Phodrang, and Sarpang (Figure 1). The study period for the term was from May to October for the years 2015–2020.

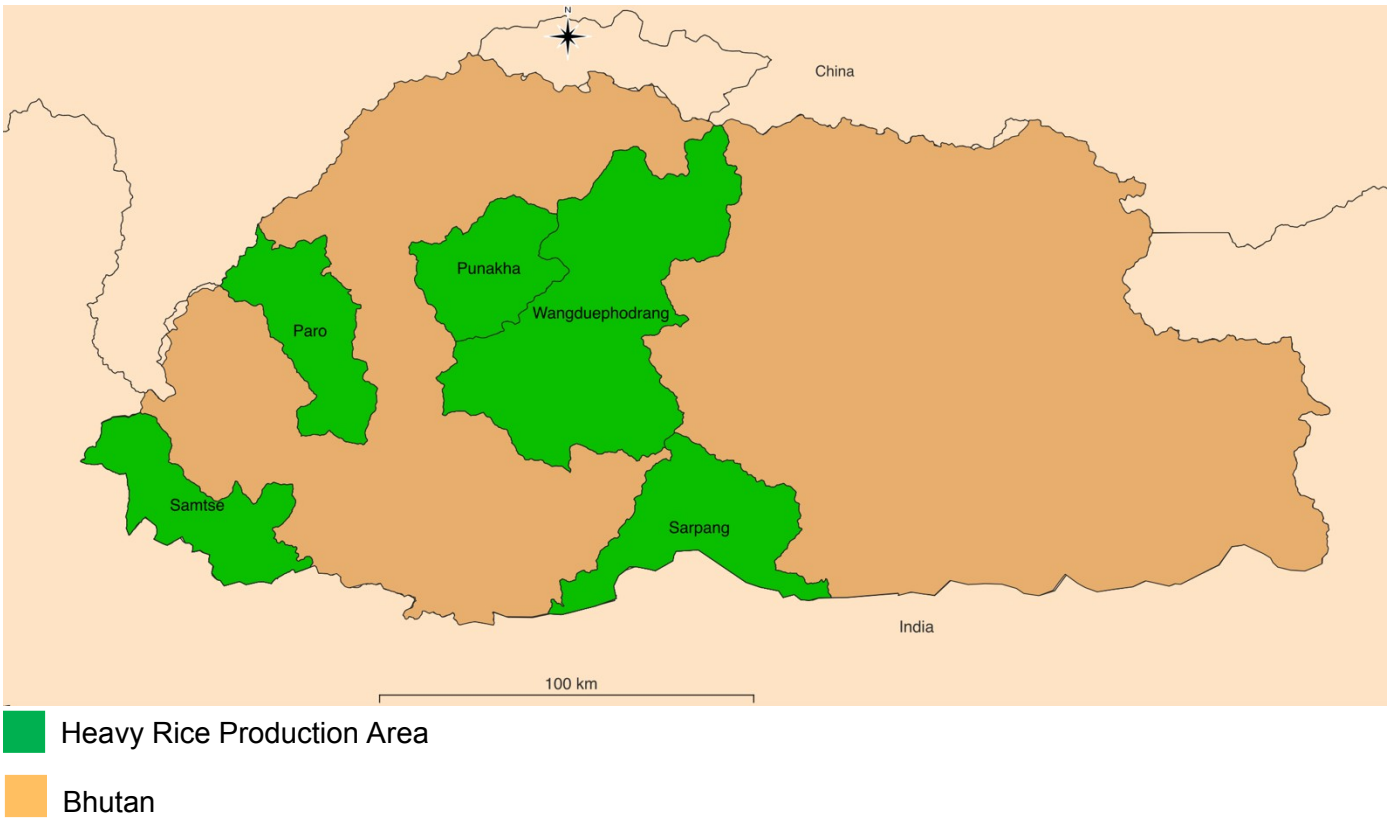

Figure 1: Study area map with heavy rice production areas outlined

2.2 Project Partners & Objectives

The team partnered with the DoA, Bhutan Foundation, and Ugyen Wangchuck Institute of Conservation and Environmental Research (UWICER) to develop a GUI that utilizes the team's crop mask information to provide a visual representation of the trends and statistics on rice distribution across Bhutan. The DoA does not currently use Earth observation data; the integration of techniques utilizing satellite remote sensing will help increase the frequency of timely agricultural assessments. The GUI will improve access and more efficiently generate rice distribution statistics (which are all based on the desired area of interest, frequency, and time frame). The Bhutan Foundation helped the team to identify appropriate points of contact within Civil Society Organizations (CSOs) and government ministries to inquire on the distribution of the project end products to different branches of government. UWICER will help engage local communities through the Himalayan Environmental Rhythm Observation and Evaluation System (HEROES) project to advocate the use of Earth observations and teach how to use the tools created by the DEVELOP team such as the GUI and sampling protocol.

3. Methodology

3.1 Data Acquisition

On CEO, the team randomly selected 1000 training points each for five heavy rice production districts; Paro, Samtse, Sarpang, Punakha, and Wangdue Phodrang. CEO uses the satellite imagery from the true colour bands of Landsat 5 TM, Landsat 7 ETM+, Aqua MODIS and Terra MODIS where sample points were collected. The Regional Land Cover Monitoring System (RLCMS) from the Hindu Kush Himalaya SERVIR hub was used as the base agricultural layer. The team also used multiple Earth observations that include Landsat 8 OLI, SRTM, and Sentinel-1 C-SAR to compute spectral indices in GEE (Table 1).

Table 1. *Instrumental datasets used in data processing*

Instrument Datasets	**Dates used**	**Source**
Landsat 8 Collection 2 Tier 1 Level 2 Surface Reflectance	Months of May to October from 2015 to 2020	Google Earth Engine (GEE)
Landsat 8 Collection 2 Tier 1 calibrated top-of-atmosphere (TOA) reflectance	Months of May to October from 2015 to 2020	GEE
Sentinel-1 C-Band Synthetic Aperture Radar (C-SAR) Ground Range Detected, log scaling data	Months of May to October from 2015 to 2020	GEE
Shuttle Radar Topography Mission (SRTM) Level 1 digital elevation data	2000-02-11 to 2000-02-22	GEE

3.2 Data Processing

Within CEO, the team manually interpreted whether the training points for the 5 major rice-producing districts were rice or non-rice. Each training point was expanded to represent a 30 m^2 plot containing 9 equidistant points of the same value, rice or not rice, to match the resolution of the Earth observation (EO) imagery. In the CEO project, the team input how confident they were on a scale from 0 to 100, with their rice classification of each training point. The training points were then imported to GEE to train the Random Forest model to classify rice crops within the study area.

In GEE, the team used Landsat 8 OLI data to compute the spectral indices of Normalized Difference Vegetation Index (NDVI), Modified Normalized Difference Water Index (MNDWI), Normalized Difference Water Index (NDWI), Soil-Adjusted Vegetation Index (SAVI), Normalized Difference Moisture Index (NDMI) and

Normalized Difference Built-up Index (NDBI). NDVI (Equation 1) and SAVI (Equation 2) outline the presence of vegetation (Gao, 1996; Huete, 1988). NDWI (Equation 3), NDMI (Equation 4), and MNDWI (Equation 5) outline the presence of water (Gao, 1996; Xu, 2006). NDBI (Equation 6) is used to outline the presence of urban and manmade built-up areas (Valdiviezo-N et al., 2017).

$$(1)\ \mathrm{NDVI} = \frac{\mathrm{NIR} - \mathrm{RED}}{\mathrm{NIR} + \mathrm{RED}}$$

$$(2)\ \mathrm{SAVI} = \frac{(\mathrm{NIR} - \mathrm{RED}) \times 1.5}{(\mathrm{NIR} + \mathrm{RED} + 0.5)}$$

$$(3)\ \mathrm{NDWI} = \frac{\mathrm{GREEN} - \mathrm{NIR}}{\mathrm{GREEN} + \mathrm{NIR}}$$

$$(4)\ \mathrm{NDMI} = \frac{\mathrm{NIR} - \mathrm{SWIR}_1}{\mathrm{NIR} + \mathrm{SWIR}_1}$$

$$(5)\ \mathrm{MNDWI} = \frac{\mathrm{GREEN} - \mathrm{SWIR}_1}{\mathrm{GREEN} + \mathrm{SWIR}_1}$$

$$(6)\ \mathrm{NDBI} = \frac{\mathrm{SWIR}_1 - \mathrm{NIR}}{\mathrm{SWIR}_1 + \mathrm{NIR}}$$

Within GEE, the team used Landsat 8 TOA data to compute Kauth-Thomas Tasseled Cap Transformation (TCT) of Greenness, Brightness, Wetness, Fourth, Fifth, and Sixth. The TCT-derived indices help to analyze and map vegetation phenology and manmade development changes over short- and long-term time periods while reducing atmospheric influences and other noise components in imagery (Baig et al., 2014). The team also used SRTM data to derive slope and elevation indices that outline the steepness of the surface (Mukul et al., 2017). The team applied both terrain correction to remove geometric distortions in the Sentinel-1 C-Band Synthetic Aperture Radar (C-SAR) imagery and a Lee-Filter to suppress speckle noise (Banerjee et al., 2021; Markert et al., 2020). The team used the modified Sentinel-1 C-SAR data to compute the indices of Vertical-Horizontal (VH) (cross-polarization), Vertical-Vertical (VV) (co-polarization), VV and VH ratio, and the normalized difference between VV and VH for both descending and ascending orbiting orientations. These indices provide information on distinctive polarization signatures at varying intensities to distinguish vegetation, overcoming the issue of clouds by using microwaves (Karjalainen et al., 2008). The Height Above Nearest Drainage (HAND), temperature, precipitation, and canopy interception were bands imported from pre-existing datasets within GEE as additional indices for crop classification. HAND outlines the vertical distance between a location and its nearest stream or drainage (Donchyts et al., 2016). Precipitation from the TerraClimate dataset outlines the precipitation accumulation in a region at a resolution of 4638.3 m (Abatzoglou et al., 2018). Temperature from ECMWF Reanalysis 5th Generation-Land (ERA5-Land) dataset outlines the temperature of the air at 2 m above the surface of land at a resolution

of 11132 m (Muñoz, 2019). Canopy Interception from the Penman-Monteith-Leuning Evapotranspiration (PML) dataset outlines the rainfall intercepted by the canopy of vegetation which successively evaporates from the leaves at a resolution of 500 m (Zhang et al., 2019).

The team created crop masks for each month of May to October from 2015 to 2020 using the Random Forest (RF) classifier within GEE. Using multiple trees in contrast to a single decision tree allows for a model which is more accurate and tolerant to noise (Breiman, 2001). For the 5000 points in the five high rice producing districts across Bhutan, the team split the points as follows: 70% for training (3500), 10% for validation (500), and the remaining for testing (1000). The team trained the RF model only on the training data by using the above-mentioned indices as features to predict the presence of rice. The held-out validation dataset was used to check the model's performance and tune the parameters as required. The team used the model to classify the testing data only after tuning and gaining sufficient confidence in the model's performance. The model's classification of the testing data serves as the primary result to quantify the model's performance.

Using weights of 0.25 for the crop masks from May to September and a weight of 0.5 for the month of October, the team aggregated the 6 crop masks to create the aggregated crop mask for a year. October was given a higher weight in contrast to other months due to rice being fully mature (which helps to distinguish rice from other vegetation better than immaturity) and ready for harvest. For the other months, rice had not fully matured for significant patterns to be captured using the indices to distinguish between rice and non-rice. The team then used the crop layer band from RLCMS (which was imported within GEE) to help filter out noise from land features such as glaciers and barren soil by clipping these regions out in the final aggregated crop mask.

3.3 Data Analysis

For each annual crop mask generated, the team produced a confusion matrix in GEE comparing the RF-predicted and CEO training point classifications of rice. A confusion matrix is a breakdown of the results of a classifier which represents the number of correct and incorrect results as true-positives, true-negatives, false-positives, and false-negatives (Zeng, 2020).

Using the confusion matrices, the team calculated several performance metrics including accuracy (Equation 7; Zeng, 2020), Cohen's kappa score (Equation 8; Pykes, 2021), precision (Equation 9), recall (Equation 10) or sensitivity (Goutte & Gaussier, 2005) and F1 score (Equation 11; Sasaki, 2007). The average of all 36 models is computed since the RF model was generated for months of May to October from 2015 to 2020.

$$(7)\ accuracy = \frac{\mathrm{TP} + \mathrm{TN}}{\mathrm{n}_{\mathrm{B}+\ \mathrm{n}_{\mathrm{G}}}}$$

$$(8)\ kappa = \frac{P_0 - P_e}{1 - P_e}$$

$$(9)\ precision(P) = \frac{TP}{TP + FP}$$

$$(10)\qquad recall(R) = \frac{TP}{TP + FN}$$

$$(11)\qquad F = \frac{2PR}{P + R}$$

The team used these metrics to quantify the model's performance on the validation data. Based on these metrics, the team tuned parameters of the RF model such as the indices used for classification and the number of decision trees in the RF model. A larger number of decision trees meant a higher number of estimators, resulting in a stronger model with less variance (Thorn, 2021; Breiman, 2001). The decision tree is made up of decision nodes that hold the threshold for an input feature such as NDVI to compare against and classify an input if it is lower or higher than this threshold value. Since we have two possible ways the input data can be classified from this node, this is referred to as the splitting of a node. There is no further splitting when we reach an end node or the leaf node where the data is classified with a positive label (rice) or negative label (non-rice). Hence, another parameter is the variables per split that specify the minimum number of features to try in creating the RF model that best classifies the training data. As we start classifying the whole dataset from the starting node in a decision tree, gradually each data point reaches a leaf node and data points that are not classified yet would be at a decision node. The minimum leaf population is a parameter that specifies the minimum number of input data at a node such that a node can be turned into a leaf node (all the input data at that node are classified). The maximum nodes parameter specifies the maximum number of leaf nodes to be generated in the RF model with a generally higher number of leaf nodes making the model less prone to noise (Thorn, 2021; Breiman, 2001). The team tuned the parameters of the model by initially generating models with different combinations of indices until we had an accuracy greater than 80%. Then the numbers for the number of decision trees, variables per split, and minimum leaf population were set from 5 to 40 in increments of 5 until we achieved a kappa score of at least 70%. Hence the team tuned the model by trying different combinations and values for the parameters using the validation data until the goal of 80% accuracy and 70% kappa score was reached.

4. Results & Discussion

4.1 Analysis of Results

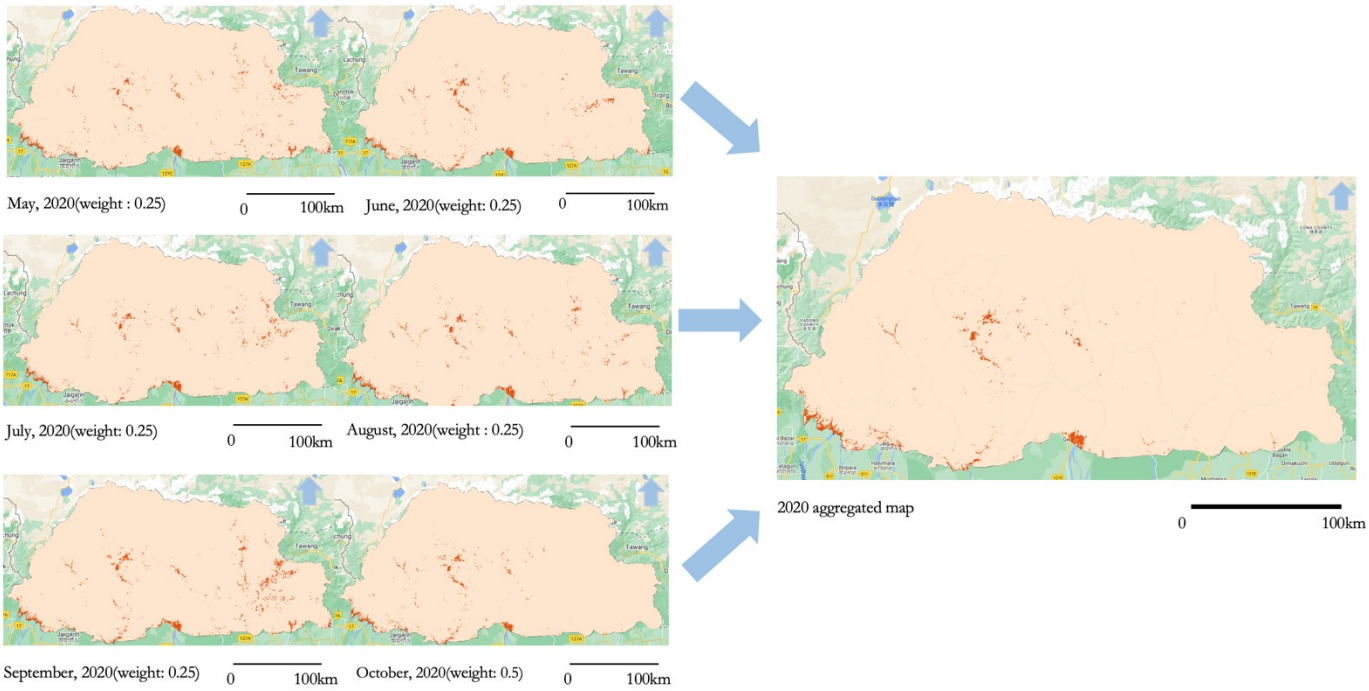

Figure 2: Monthly aggregated maps with weights for 2020

The darker orange pixels on the maps in the figure above represents the rice paddy fields whereas areas with the lighter shade of orange are the non-rice areas picked up by the RF model. The dark orange area cover is referred to as a rice mask. A rice mask is a layer which identifies rice areas on the ground using satellite imagery and mathematical classification techniques coupled with field data.

The six maps on the left of *Figure 2* show the rice mask layers for May to October of 2020 to which individual weights are applied and aggregated to create an annual map of 2020 which is the map on the right.

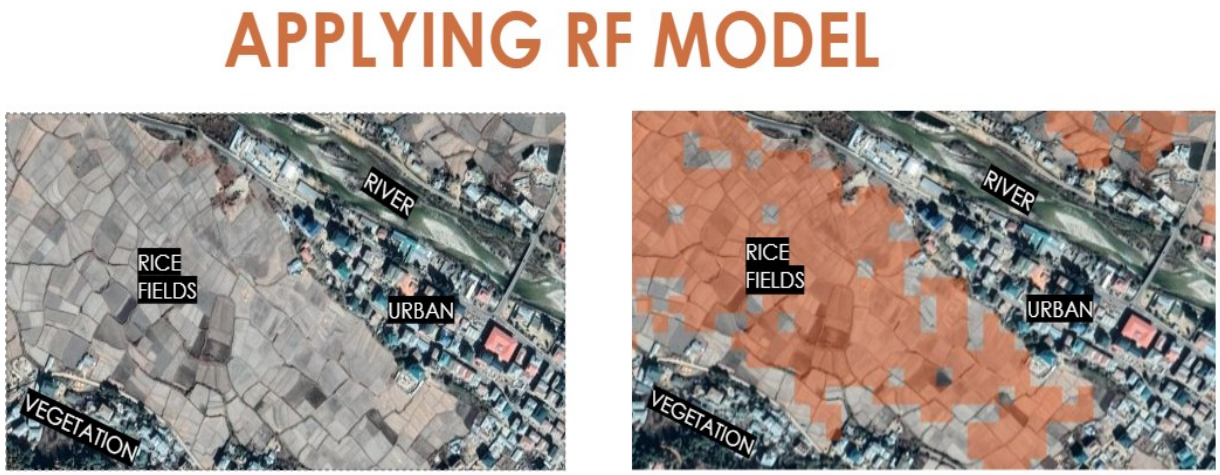

Figure 3: Applying RF model to an area in Paro. The crop mask for rice fields is shown in orange.

As an example of a better view of how the random forest model performs, figure 3 displays the classification of the model in the region of Paro for 2020. The images to the left of figure 2 show the satellite view of zoomed area. The image to the right shows the same area, but displays the aggregated rice mask layer of 2020 created by our random forest model. The RF model highlights most of the paddy fields in that area in orange while ignoring most of the non-rice areas such as the water bodies – river, urban structures, and some non-rice vegetation. However, there are a few rice areas which the rice mask does not include. This could be because the model has not learned robust patterns to classify these areas as rice or a caveat of using the RLCMS layer to clip out other types of non-rice land features.

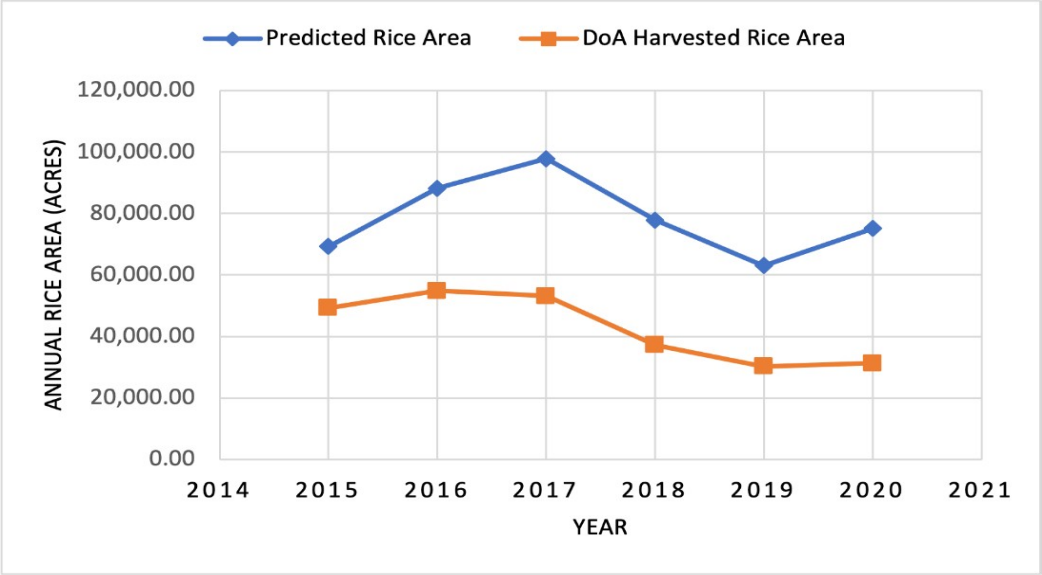

Figure 4: The graph shows the predicted rice area in acres and the harvested rice area according to the DoA statistics in the whole of Bhutan from 2015 to 2020.

After the team developed the aggregated crop mask for each year from 2015 to 2020 in all the districts of Bhutan, in GEE all the pixels of the crop mask were aggregated and converted to acres. The model predicted an increase in rice area from 2015 to 2017, but a gradual decrease till 2019 before increasing again in 2020. The model also predicted 2019 to have the lowest rice area of 63,098 acres and 2017 to have the highest rice area of 97,789 acres. In comparison to the actual statistics recorded by the DoA, these predictions overclassify regions as rice. 2016 was the actual year with the highest rice area, but the overall trend in annual rice area is consistent. The discrepancy could result from the model predicting all areas that holds rice, whereas the statistics from the department denote the amount of harvested rice area only.

Within GEE, the team computed the confusion matrices using the testing set.

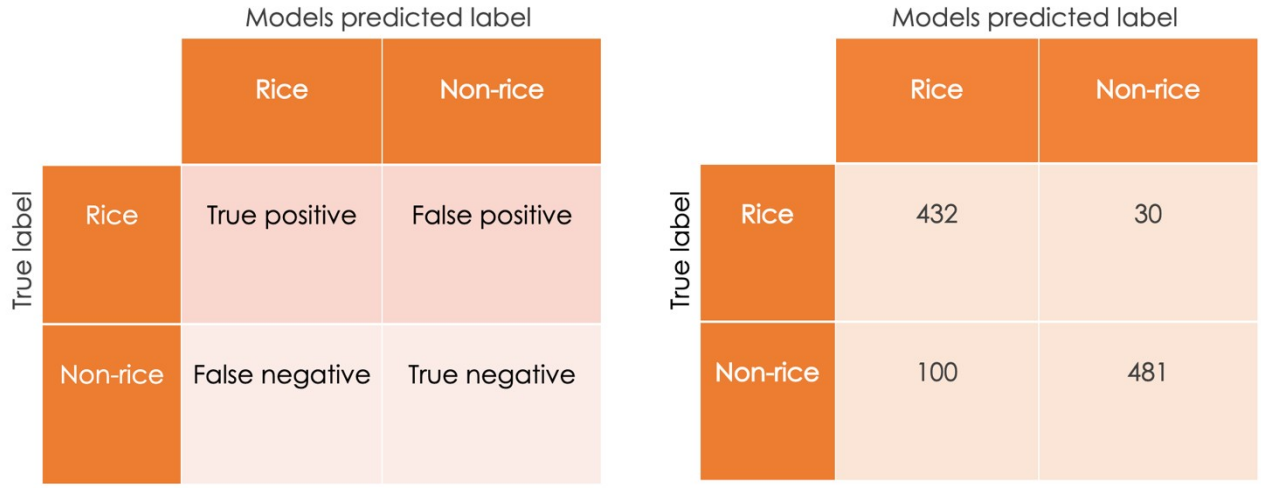

Figure 5: Confusion matrices with average number of true positives, true negatives, false positives and false negatives for all RF models generated.

As shown in figure 5, the RF model identified 432 rice points and 481 non-rice points correctly. The RF model misclassified 30 points as rice and 100 points as non-rice. The confusion matrices show that the RF model performs worse in identifying non-rice areas in comparison to rice areas. A machine learning model is only as powerful as the amount and quality of data that it has been trained on, so with the current set of training data, the regions are heavily skewed to the western regions of Bhutan. This means that there are specific rice patterns in the indices measured that are not captured by the RF model. Also, as the training points are randomly generated within western Bhutan in CEO, it is plausible that not all the generated points are extensive in encompassing information about all forms of paddy fields, rice species and non-rice features. Certain characteristics of other non-rice crops or vegetation measured by the indices may also overlap with rice which introduces erroneous patterns into the model. To test the validity of our crop mask, within GEE the team computed statistical measurements for all the prediction results from the confusion matrices and they were averaged (Table 2). The team used the 1000 testing points from CEO as the testing set for the RF model and found the accuracy score of our model when distinguishing between rice and non-rice areas to be 85.9%, the F1 score to be 85.1% and the Cohen Kappa score to be 71.8%.

Table 2: Statistical measurements from GEE

Statistic Method	Random Forest
Accuracy Score	85.9
F1 score	85.9
Cohen Kappa Score	71.8

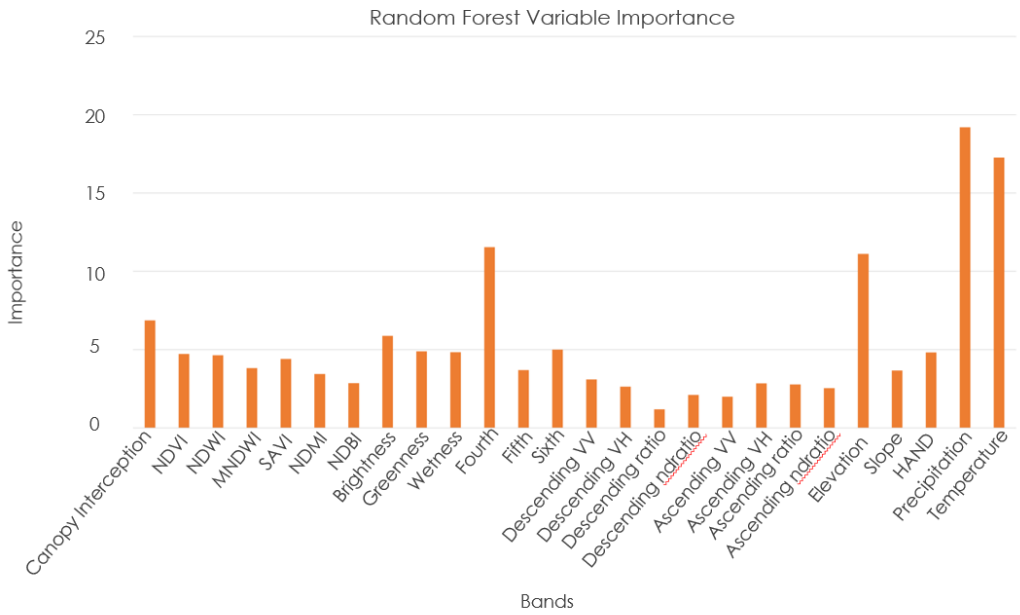

Figure 6: Comparison of indices' importance in the RF model.

Figure 6 represents the level of importance of the variables (e.g., the level of contribution of the spectral indices in distinguishing rice and non-rice points as perceived by the model in generating the crop mask). The model picked up on elevation as a key driver in the classification problem which could be due to the different rice ecosystems of Bhutan that are distinguished by the three altitudes of low, mid, and high. Precipitation and temperature were also considered important for the model which could be due to each rice ecosystem having its own optimal precipitation and temperature which are essential for rice growth. The Tasseled Cap Transformation of Fourth's high importance could be due to the distinct vegetation phenology and urban development changes detected around the rice fields. Other indices had relatively equal levels of importance. As there is no specific index for rice identification, we can see that our model uses an integration of various other indices.

4.2 Limitations

In using satellite imagery, it is possible that the images and bands used to capture the rice fields are not uniform. The general environment of the district and when the image was captured introduce diversity on what the random forest model considers to be rice. Also, our model was trained with respect to the growing period of 2015 to 2020, so the indices used are specific to that time period. Since these conditions could change, the patterns learned by the model may not perform well on other time periods. To reiterate, the model is only as powerful as the amount and variation of data that it has been trained on, hence, further work is needed to validate the significance of the findings.

The random forest model is an ensemble of multiple decision trees that learn a specific pattern in the values of indices used to label a point as rice, but this is

difficult to interpret with multiple indices. Hence, it is difficult to isolate a single study variable and determine the significance of each variable for rice classification.

Our model currently assumes that all rice crops are of a single variety although there are multiple varieties grown in different ecosystems and climatic conditions. This is a generalization made for the ease of creating a general crop mask which also makes it difficult for the model to learn a consistent pattern to classify a point as rice, as points labelled as rice may have stark differences in terms of measured indices (like in the case of rice from terraced slopes at high altitude in contrast to rice from the flat southern foothills).

Human errors such as bias and random errors may have occurred in the collection of rice plots in CEO and the in-field points provided by the DoA. Errors in this reference data dictate the points that the model was trained on and ultimately the pattern learned. It is also important to note that the randomness in the initial collection of points and the splitting of the data influences the patterns learned by the RF model and its accuracy.

4.3 Future Work

The third term project could work on expanding the GUI created by this project team to determine the soil productivity and yield of crops in the different districts of Bhutan. The continuation project could also work on distinguishing abandoned farmlands from active agricultural lands in satellite imagery. The third term could also bolster the crop mask to identify not just rice, but different variations that are grown specific to each region. These end products will assist partners in making the required decisions for the agricultural challenges faced in Bhutan.

5. Conclusions

The team expanded on the previous term's RF model by tuning the parameters and collecting 5000 points for the five major rice producing districts of Bhutan. The RF model had an accuracy score of 85.9 and kappa score of 71.8. The model predicted an increase in rice area from 2015 to 2017, but a gradual decrease till 2019 before increasing again in 2020. The model also predicted 2019 to have the lowest rice area of 63,098 acres and 2017 to have the highest rice area of 97,789 acres. In comparison to the actual statistics recorded by the department of agriculture, these predictions display disparity by overclassifying regions, and 2016 was the actual year with the highest rice area but the overall trend in annual rice area is consistent. The team also updated the sampling protocol from the previous term with additional information on how to work with the CEO. With the updated sampling protocol, the partners will also be able to become familiar with the CEO so they can create projects to collect various training points for different regions in the country.

The GUI created by the team will be beneficial to partners as the partners will not necessarily have to be familiar with GEE and programming when using it. The end users will only need to select their region of interest from the country to be able to produce different results and graphs. The end users can compare the harvested rice area from their in-situ data to the rice area in Bhutan calculated by our model. The end users can also get to know the rice distribution in acres either on district

level or sub-district level. The GUI also has graphs with precipitation, temperature, and soil moisture trends over the years. Partners can view the importance of those variables, which have direct or indirect impacts on their agricultural statistics over the years. The graphs can also assist partners in determining the relationship of those variables with agriculture on a single interface.

6. Acknowledgments

The team would like to thank everyone mentioned below for helping us make the project successful:

- Tim Mayer (NASA SERVIR Science Coordination Office)
- Filoteo Gomez-Martinez (NASA SERVIR Science Coordination Office)
- Biplov Bhandari (NASA SERVIR Science Coordination Office)
- Meryl Kruskopf (NASA SERVIR Science Coordination Office)
- Stephanie Jimenez (NASA SERVIR Science Coordination Office)
- Kaitlin Walker (NASA SERVIR Science Coordination Office)
- Micky Maganini (NASA SERVIR Science Coordination Office)
- Sean McCartney (NASA Goddard Space Flight Center)
- Dr. Kenton Ross (NASA Langley Research Center)
- Dr. Robert Griffin (The University of Alabama Huntsville)
- Dr. Jeffry Luvall (NASA Marshall Space Flight Center)
- Paxton LaJoie (NASA DEVELOP - Marshall Space Flight Center)
- Tshering Wangchen (Bhutan Department of Agriculture)
- Nidup Dorji (Bhutan Department of Agriculture)

This material contains modified Copernicus Sentinel data (2015-2020), processed by ESA.

Any opinions, findings, and conclusions or recommendations expressed in this material are those of the author(s) and do not necessarily reflect the views of the National Aeronautics and Space Administration.

This material is based upon work supported by NASA through contract NNL16AA05C.

7. Glossary

Accuracy – The ratio of correct predictions and it is calculated by the sum of true negatives and true positives divided by the total number of events.
CEO – Collect Earth Online. An open-source system that can be used for projects requiring land cover and/or land use reference data.
Cohen's kappa score – The comparison of the probability of agreement (P_o) to the random probability agreement (P_e).
C-SAR – C-band Synthetic Aperture Radar instrument provides an all-weather, day and night imaging capability to capture measurement data at high and medium resolutions for land, coastal zones, and ice observations.
Earth observations – Satellites and sensors that collect information about the Earth's physical, chemical, and biological systems over space and time.
ETM+ – Enhanced Thematic Mapper Plus instrument provides multispectral high-resolution imaging information of the Earth's surface.
F1 score – Is the average of precision and recall.

Gewogs – Smaller territorial divisions under the 20 districts.
Google Earth Engine (GEE) – A cloud-based geospatial processing platform that combines multi-petabyte catalog of satellite imagery and geospatial datasets with planetary-scale analysis capabilities.
NDMI – Normalized Difference Moisture Index. Ratio between the difference and the sum of the refracted radiation in near infrared and short infrared.
NDVI – Normalized Difference Vegetation Index. Ratio between the difference and the sum of the near infrared and visible reflectance of vegetation.
NDWI – Normalized Difference Water Index. The ratio between the difference and the sum of near infrared and green channels.
OLI – Operational Land Imager, uses long detector arrays with over 7000 detectors per spectral band, aligned across its focal plane to view across the swath.
Polarization – Polarization refers to the direction of travel of an electromagnetic wave vector's tip.
Polarization signatures – In changing the polarization of the transmitted signal and receiving several different polarized images from the same series of pulses, SAR systems provide details on the polarimetric properties of the observed surface.
Precision – Determines the accurate prediction for the positive classes.
Random Forest (RF) – A supervised learning method that is a combination of decision trees where every tree classifies inputs based on random features and the label predicted by the majority of trees is the classification of the input.
Recall or sensitivity – Provides the ratio of predicted positive classes.
RLCMS – The Regional Land Cover Monitoring System is a functioning system to create annual land cover maps and detect land cover changes.
SRTM – Shuttle Radar Topography Mission was an international project, led by NASA and the National Imagery and Mapping Agency (NIMA), to create a digital elevation model on a near global scale to generate a high resolution digital topographic database of Earth.

8. References

Abatzoglou, J. T., Dobrowski, S. Z., Parks, S. A., & Hegewisch, K. C. (2018). TerraClimate, a high-resolution global dataset of monthly climate and climatic water balance from 1958–2015. Scientific Data, 5(1). https://doi.org/10.1038/sdata.2017.191

Baig, M. H. A., Zhang, L., Shuai, T., & Tong, Q. (2014). Derivation of a tasselled cap transformation based on Landsat 8 at-satellite reflectance. *Remote Sensing Letters*, *5*(5), 423–431. https://doi.org/10.1080/2150704x.2014.915434

Banerjee, S., Sinha Chaudhuri, S., Mehra, R., & Misra, A. (2021). A Survey on Lee Filter and Its Improved Variants. Advances in Smart Communication Technology and Information Processing, 371–383. https://doi.org/10.1007/978-981-15-9433-5_36

Breiman, L. (2001). Random Forests. *Machine Learning*, *45*(1), 5–32. https://doi.org/10.1023/a:1010933404324

Chhogyel, N., & Kumar, L. (2018). Climate change and potential impacts on agriculture in Bhutan: A discussion of pertinent issues. *Agriculture & Food Security*, *7*(1). https://doi.org/10.1186/s40066-018-0229-6

Dolma, S., Dorji, W., Khandal, K., & Seldon, Y. (2021). Bhutan Agriculture I: Developing a crop mask for rice and creating a data collection protocol utilizing remotely sensed data in Bhutan [Unpublished manuscript]. NASA DEVELOP National Program, Alabama – Marshall.

Donchyts, G., Winsemius, H., Schellekens, J., Erickson, T., Gao, H., Savenije, H., & van de Giesen, N. (2016). Global 30m Height Above the Nearest Drainage. NASA ADS, 18, EPSC2016-17445. https://ui.adsabs.harvard.edu/abs/2016EGUGA.1817445D/abstract

European Space Agency. Copernicus Open Access Hub (2015-2021). *Sentinel 1 C-Synthetic Aperture Radar* [Data set]. ESA. https://sentinels.copernicus.eu/web/sentinel/user-guides/sentinel-1-sar

European Space Agency. Copernicus Open Access Hub (2020). *Sentinel 2A and 2B Multispectral Instrument (MSI)* [Data set]. ESA. https://sentinels.copernicus.eu/web/sentinel/technical-guides/sentinel-2-msi

Farr, T.G., Rosen, P.A., Caro, E., Crippen, R., Duren, R., Hensley, S., Kobrick, M., Paller, M., Rodriguez, E., Roth, L., Seal, D., Shaffer, S., Shimada, J., Umland, J., Werner, M., Oskin, M., Burbank, D., & Alsdorf, D.E. (2007). *The Shuttle Radar Topography Mission: Reviews of Geophysics* (v45, no. 2) [RG2004]. NASA/USGS/JPL-Caltech. Retrieved from https://doi.org/10.1029/2005RG000183

Gao, B. (1996). NDWI—A normalized difference water index for remote sensing of vegetation liquid water from space. *Remote Sensing of Environment*, *58*(3), 257–266. https://doi.org/10.1016/s0034-4257(96)00067-3

Gorelick, N., Hancher, M., Dixon, M., Ilyushchenko, S., Thau, D., & Moore, R. (2017). Google Earth Engine: Planetary-scale geospatial analysis for everyone. *Remote Sensing of Environment,* 202,18-27. https://doi.org/10.1016/j.rse.2017.06.031

Goutte, C., & Gaussier, E. (2005). A probabilistic interpretation of precision, recall and F-score, with implication for evaluation. *Lecture Notes in Computer Science*, 345–359. https://doi.org/10.1007/978-3-540-31865-1_25

Huete, A. R. (1988). A soil-adjusted vegetation index (SAVI). *Remote Sensing of Environment*, *25*(3), 295–309. https://doi.org/10.1016/0034-4257(88)90106-X

Karjalainen, M., Kaartinen, H., & Hyyppä, J. (2008). Agricultural monitoring using Envisat alternating polarization SAR images. *Photogrammetric Engineering & Remote Sensing*, *74*(1), 117–126. https://doi.org/10.14358/pers.74.1.117

MacroTrends. (n.d.). *Bhutan arable land 1961-2022*. Retrieved from https://www.macrotrends.net/countries/BTN/bhutan/arable-land

Markert, K. N., Markert, A. M., Mayer, T., Nauman, C., Haag, A., Poortinga, A., Bhandari, B., Thwal, N. S., Kunlamai, T., Chishtie, F., Kwant, M., Phongsapan, K., Clinton, N., Towashiraporn, P., & Saah, D. (2020). Comparing Sentinel-1 surface water mapping algorithms and radiometric terrain correction processing in Southeast Asia utilizing Google Earth Engine. *Remote Sensing*, *12*(15), Article 2469. https://doi.org/10.3390/rs12152469

Mukul, M., Srivastava, V., Jade, S., & Mukul, M. (2017). Uncertainties in the Shuttle Radar Topography Mission (SRTM) heights: Insights from the Indian Himalaya and Peninsula. *Scientific Reports*, *7*(1). https://doi.org/10.1038/srep41672

Muñoz Sabater, J., (2019): ERA5-Land monthly averaged data from 1981 to present. Copernicus Climate Change Service (C3S) Climate Data Store (CDS). https://doi.org/10.24381/cds.68d2bb30

National Plant Protection Center (NPPC). Pests of Bhutan. (n.d.). Retrieved June 28, 2022, from https://pestsofbhutan.nppc.gov.bt/crop-and-pest-identification/wildlife-vertebrate-pests/wild-boars/

Parker, L., Guerten, N., Nguyen, T. T., Rinzin, C., Tashi, D., Wangchuk, D., Bajgai, Y., Subedi, K., Phuntsho, L., Thinley, N., Chhogyel, N., Gyalmo, T., Katwal, T. B., Zangpo, T., Acharya, S., Pradhan, S., & Penjor, S (2017). Climate change impacts in Bhutan: Challenges and opportunities for the agricultural sector. *CCAFS Working Paper no. 191.* Wageningen, Netherlands: CGIAR Research Program on Climate Change, Agriculture and Food Security (CCAFS).

Pykes, K. (2021). *Cohen's kappa*. Medium. Retrieved July 5, 2022, from https://towardsdatascience.com/cohens-kappa-9786ceceab58

Sasaki, Y. (2007, October 26). The truth of the F-measure. Retrieved July 5, 2022, from https://cs.odu.edu/~mukka/cs795sum10dm/Lecturenotes/Day3/F-measure-YS-26Oct07.pdf

SERVIR GLOBAL. (n.d.). Regional Land Cover Monitoring System - Hindu Kush Himalaya. *Service Catalogue.* Retrieved June 30, 2022, from https://www.servirglobal.net/ServiceCatalogue/details/5bc986a651ebdcae79683361

The World Bank. (n.d.). *Agriculture, forestry, and fishing, value added (% of GDP) - Bhutan*. [Data Set]. The World Bank. Retrieved August 10, 2022, from https://data.worldbank.org/indicator/NV.AGR.TOTL.ZS?locations=BT

The World Bank. (2022). *The World Bank in Bhutan*. The World Bank. https://www.worldbank.org/en/country/bhutan

Thorn, J. (2021). *Random Forest: Hyperparameters and how to fine-tune them*. Medium. Retrieved July 5, 2022, from https://towardsdatascience.com/random-forest-hyperparameters-and-how-to-fine-tune-them-17aee785ee0d

Tobden, T., Subbha, M., Yangzom, T., Penjor, S., Dorji, R., Wangmo, K., & Tenzin, K. (2021). *Agriculture statistics 2020*. Ministry of Agriculture and Forests, Directorate Services, Renewable Natural Resources Statistics Division. https://www.doa.gov.bt/wp-content/uploads/2021/08/Agriculture-Statistics-2020.pdf

Tshewang, S., Park, R., Chauhan, B., & Joshi, A. (2018). Challenges and Prospects of Wheat Production in Bhutan: A Review. *Experimental Agriculture*, *54*(3), 428–442. https://doi.org/10.1017/S001447971700014X

USGS (1999). *USGS Landsat 7 Level 2, Collection 2, Tier 2* [Dataset]. USGS. Retrieved from https://developers.google.com/earth-engine/datasets/catalog/LANDSAT_LE07_C02_T2_L2?hl=en

USGS (2013). *USGS Landsat 8 Collection 2, Tier 1* [Dataset]. USGS. Retrieved from https://doi.org/10.3390/rs61111244

USGS (2013). *USGS Landsat 8 Collection 2, Tier 1 TOA Reflectance* [Dataset]. USGS/Google. Retrieved from https://www.usgs.gov/landsat-missions/landsat-collections

Valdiviezo-N, J. C., Téllez-Quiñones, A., Salazar-Garibay, A., & López-Caloca, A. A. (2017). Built-up index methods and their applications for urban extraction from Sentinel 2A satellite data: Discussion. *Journal of the Optical Society of America A*, *35*(1), Article 35. https://doi.org/10.1364/josaa.35.000035

World Bank. (2017). *Climate-smart agriculture in Bhutan - World Bank*. Climate Change Knowledge Portal. Retrieved from https://climateknowledgeportal.worldbank.org/sites/default/files/2019-06/CSA-in-Bhutan.pdf

Xu, H. (2006). Modification of normalized difference water index (NDWI) to enhance open water features in remotely sensed imagery. *International Journal of Remote Sensing*, *27*(14), 3025–3033. https://doi.org/10.1080/01431160600589179

Zeng, G. (2020). On the confusion matrix in credit scoring and its analytical properties. *Communications in Statistics - Theory and Methods*, *49*(9), 2080–2093. https://doi.org/10.1080/03610926.2019.1568485

Zhang, Y., Kong, D., Gan, R., Chiew, F.H.S., McVicar, T.R., Zhang, Q., & Yang, Y., (2019). Coupled estimation of 500m and 8-day resolution global

evapotranspiration and gross primary production in 2002-2017. Remote Sens. Environ. 222, 165-182. https://doi.org/10.1016/j.rse.2018.12.031